Patrick Wiegand\*, Fatih Ilgaz, Benjamin Spetzler, Robert Rieger

# Extended mBvD Model for MEMS Delta-E **Magnetic Field Sensors**

https://doi.org/10.1515/cdbme-2025-0148

**Abstract:** In this paper, thin film magnetoelectric resonators are used to underpin an extension to the (modified) Butterworth-van Dyke (mBvD) model. These resonator types are being investigated for applications in the bio-medical domain for e.g., movement analysis or localization by sensing magnetic fields. The mBvD model provides an electrical equivalent circuit for such resonators, enabling the analysis of their response to applied currents or voltages. However, the resonators studied here change their properties - specifically, their resonance frequency - when exposed to a magnetic field. To better understand this behavior and adapt the resonator sensors to (medical) applications, the mBvD model is extended to include this property. Thus, to reflect the changes in the mBvD model, a dependency between the electrical components and the surrounding magnetic field is introduced. It is shown, that 4<sup>th</sup> order polynomial functions are suitable to map the changes and provide a robust model.

Keywords: Magnetic field sensor, MEMS resonator, delta-E effect, mBvD model, equivalent electrical circuit.

## 1 Introduction

Microelectromechanical system (MEMS) magnetic field sensors have shown to be usable for magnetic fields in the sub nano-Tesla range and to have a high spatial resolution [1,2]. They can be used in a wide variety of applications including biomedical applications, e.g., healthcare [3,4], motion tracking [5] or object localisation [6]. This offers usability for medical treatments and diagnosis like movement analysis or tracking surgical tools inside the human body.

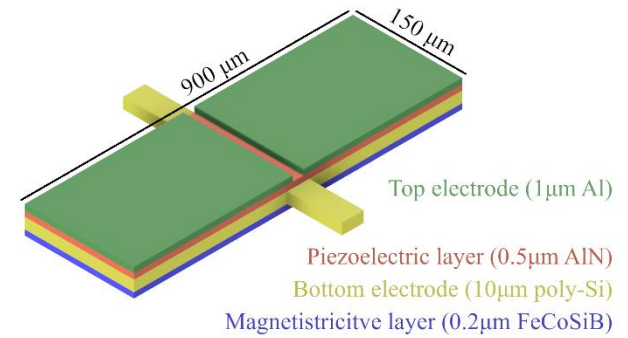


Figure 1: The resonator used in this paper is a cantilever measuring 900 µm x 150 µm. It is clamped in the middle of its long axis. The thickness of the used layers is given in parentheses.

Here, a MEMS resonator with a thin film magnetostrictive layer is used to measure magnetic fields. To characterize resonant sensors, the (modified) Butterworth-van Dyke (mBvD) [7] model is often used. The mBvD model represents the physical behaviour of the resonator as an equivalent electrical circuit. With this circuit model, resonator characteristics and the electrical behaviour can be described. Based on this, external circuitry can be adapted to the found resonator characteristics and simulation of a whole sensor system becomes possible.

## 2 Sensor

The MEMS resonators used are double wing resonators with a clamping in the middle of the long axis of a free-standing beam. They measure 150 µm x 900 µm as shown in Fig. 1. The resonator consists of four thin film layers. From bottom to top these are: A magnetostrictive layer made of (Fe<sub>90</sub>Co<sub>10</sub>)<sub>78</sub>Si<sub>12</sub>B<sub>10</sub> (FeCoSiB, 0.2-µm thick), which is used as the sensing element, as it changes its stiffness due to magnetic fields, a silicon layer (10-µm thick) as a bottom electrode, a piezoelectric layer (AlN, 1-µm thick) to excite and read out the cantilever and a top electrode made of aluminium (1-µm thick). The resonators are produced in a commercially available process, while the magnetostricive layer is applied at Kiel University [8].

<sup>\*</sup>Corresponding author: Patrick Wiegand: Department of Electrical and Information Engineering, Kiel University, Kaiserstraße 2, Kiel, Germany, e-mail: pw@tf.uni-kiel.de 2nd Author Fatih Ilgaz, 3rd Author Bejamin Spetzler: Department of Materials Science, Kiel University, Kiel, Germany 4th Author Robert Rieger: Department of Electrical and Information Engineering, Kiel University, Kiel, Germany

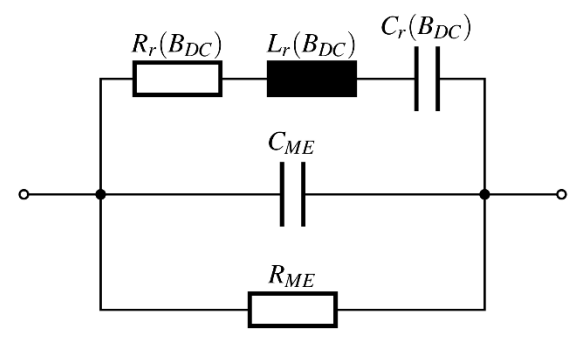


Figure 2: The electrical equivalent circuit of the mBvD model consists of a resonant RLC series tank, parallel to  $C_{ME}$  and  $R_{ME}$ . The RLC tank components of the resonator used in this paper depend on the magnetic field  $B_{DC}$ .

To measure magnetic fields, the delta-E effect is exploited [9,10]. When a magnetostrictive material, such as FeCoSiB, is introduced to a magnetic field, it changes its elasticity and thus, its elastic modulus E. In case of the presented resonator, a change of the elastic modulus E of the FeCoSiB layer leads to a shift of the resonator's resonance frequency  $f_r$ . This shift can be detected by measuring the resonator's impedance Z. Therefore, the resonator is electrically excited at its resonance frequency  $f_r$  at a given magnetic field  $B_{DC}$  with an alternating voltage  $u_{ex}$ . By measuring the current  $i_0$  through the resonator, the impedance can be calculated. If a magnetic signal  $B_{AC}$  is superimposed to the static magnetic field  $B_{DC}$  and the electric excitation frequency  $f_{ex}$  is kept constant, this leads to a change of the measured current  $i_o$ . In the time domain, this is visible as an amplitude modulation of the current  $i_o$ . For the resonators used, this method can measure magnetic frequencies up to 1kHz and magnetic amplitudes as low as 7 nT [1].

## 3 Sensor Model

The mBvD model is an equivalent electrical circuit used to represent the electrical and mechanical properties of a resonator. It consists of an RLC series tank  $(R_r, L_r, C_r)$  parallel to a resistor  $R_{ME}$  and a capacitance  $C_{ME}$ , as shown in Fig. 2.  $R_{ME}$  and  $C_{ME}$  can be attributed to the AlN layer as piezoelectric

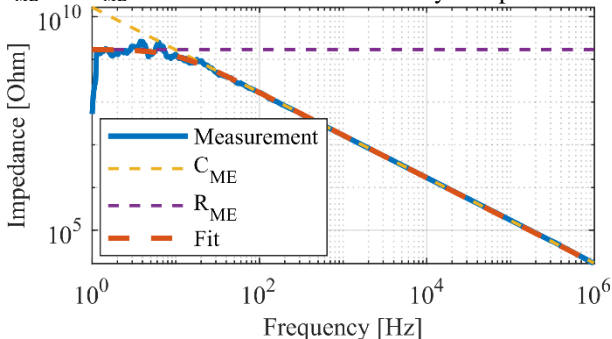


Figure 3: With the measurement over a broad frequency range from 1 Hz to 1 MHz a fit for for  $C_{ME}$  and  $R_{ME}$  can be found.

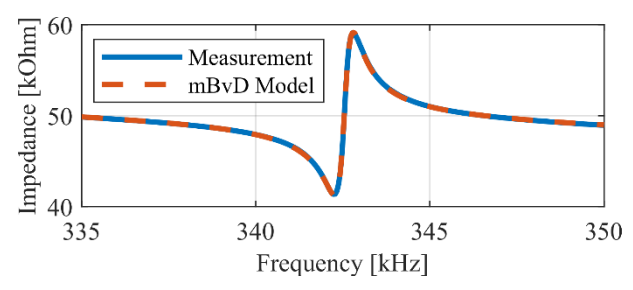


Figure 4: The impedance measurement and mBvD simulation match well for the resonator. This measurement was taken at  $B_{\rm DC}$  = -0.72 mT.

loss ( $R_{ME}$ ) and piezoelectric capacitance ( $C_{ME}$ ), while the RLC tank describes the resonating behaviour.

The model works well to analyse noise sources [11,12] or compare resonators [13] and has been adapted for many other applications [14,15]. By adding or leaving out parts of the model it can be customized to model different problems. However, since all these models employ constant values for the electric components of the equivalent circuit, they cannot take into account a change of the resonator. For the resonator presented here, this change is due to the delta-E effect.

It is not possible to retrieve the magnetic sensitivity directly from a single model fit. Instead, to calculate the magnetic sensitivity, multiple mBvD fits with varying magnetic fields  $B_{DC}$  are measured. The derivative of the resonance frequency change across these fits then yields the desired sensitivity [8].

Here, we present an approach to extend the mBvD model by including a dependency on a magnetic field  $B_{DC}$ . Since  $R_{ME}$  and  $C_{ME}$  are given by the geometry of the resonator, due to the electrodes forming a leaky capacitor with the piezoelectric layer, these values are not impacted by magnetic field changes. In contrast, the resonance frequency of the resonator changes with the magnetic field. Therefore, the RLC tank branch and thus,  $R_r$ ,  $L_r$  and  $C_r$  depend on  $B_{DC}$ . In the following, it is shown that the behaviour of the RLC tank components can be represented well by fourth-order polynomial functions.

As of now, the model is designed for an excitation voltage amplitude of 100 mV. In principle, it can be adjusted to other amplitudes as well, as long as additional nonlinearities due to excitation amplitude variation are of no concern.

### 4 Measurement

To fit the mBvD model properly, impedance measurements over frequency are necessary. The measurements are done with a lock-in amplifier (MFLI, Zurich instruments, Switzerland) and conducted in an electrically and magnetically

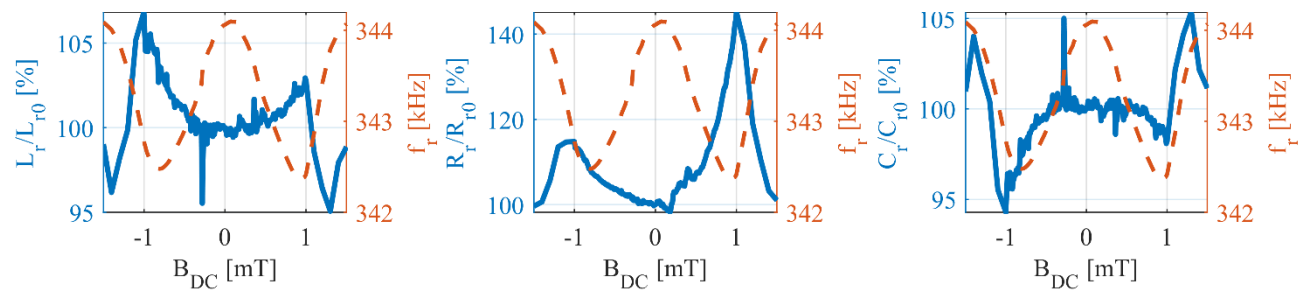


Figure 5: In blue, the values of  $C_r$ ,  $R_r$  and  $L_r$  at varying magnetic fields  $B_{DC}$  are drawn. The curves are normalized to their corresponding values  $C_{r0}$ ,  $R_{r0}$  and  $L_{r0}$  at  $B_{DC} = 0$  T. The dashed red lines show the resonance frequency  $f_r$ .

shielded chamber. The shielding setup is described in detail in [16]. To generate different magnetic fields, a constant current source (B2962a, Keysight Technologies, USA) is used together with a coil. The resonator is placed inside this coil to obtain a homogeneous magnetic field. The voltage output of the lock-in amplifier is set to an amplitude of  $u_{ex} = 100 \text{ mV}$  and excites the resonator while the current input is used to measure the current  $i_o$  through the resonator. By dividing the excitation amplitude  $u_{ex}$  by the measured current amplitude  $i_o$ , the relevant real part of the resonator impedance Z is obtained.

Measuring the impedance across a wide frequency range from 1 Hz to 1 MHz, the values for  $R_{ME}$  and  $C_{ME}$  can be deduced, as shown in Fig. 3. Additional measurements with higher frequency resolution in the vicinity of the resonance frequency are made. Here, the values for  $C_r$ ,  $R_r$  and  $L_r$  can be found with an iterative fitting algorithm. This yields a complete electric equivalent circuit matching the sensor very well, as the comparison between model and measurement in Fig. 4 shows for a randomly selected measurement with  $B_{DC} = -0.72$  mT.

Measuring impedance curves at different magnetic fields  $B_{DC}$  from -1.5 mT to 1.5 mT yields varying values for  $C_r$ ,  $R_r$  and  $L_r$  as the resonance frequency of the resonator changes and thus the RLC tank impedance changes.

# 5 Analysis

The mBvD values obtained for the  $C_r$ ,  $R_r$  and  $L_r$  are shown in Fig. 5. Between -1 mT and 1 mT they change continuously,

before dropping/rising suddenly outside of this interval. However, the most relevant operating points of the resonator are given inside of this interval, namely at the steepest points of the resonance frequency curve. Those occur at approximately  $\pm 0.5$  mT. Therefore, the analysis of the model should be restricted to values inside of this interval. As shown in Fig. 6, the measurement fits can be approximated well with a polynomial function of  $4^{th}$  order. A polynomial function was chosen, as it is easy to implement in many simulation environments. The  $4^{th}$  order strikes a favourable balance between computational effort and a good match with the measurements.

To test this extended model, two signal measurements are compared to simulations. In one case, a static magnetic field  $B_{DC} = 0.43$  mT is used to bias the resonator to an operating point where the magnetic sensitivity is maximized. In the other case, no  $B_{DC}$  field is applied. The resonator is excited with a voltage of  $u_{ex} = 100$  mV at  $f_{ex} = 343.17$  kHz (resonance frequency for this bias point), respective at  $f_{ex} = 344.09$  kHz in the case without  $B_{DC}$ . Additionally, the magnetic field  $B_{DC}$  is superimposed with a magnetic sinusoidal test signal at  $f_{Bac} = 10$  Hz with a field amplitude of  $B_{AC} = 1$   $\mu$ T.

Both cases show a good match with the provided model in Fig. 7. The difference in amplitude at the carrier and signal peaks is approximately a factor of two in the worst case. The increased noise floor of the measurement at the magnetic working point is due to the noise of the current source providing the current to the  $B_{DC}$  coil, which is switched off for the measurement without a  $B_{DC}$  field.

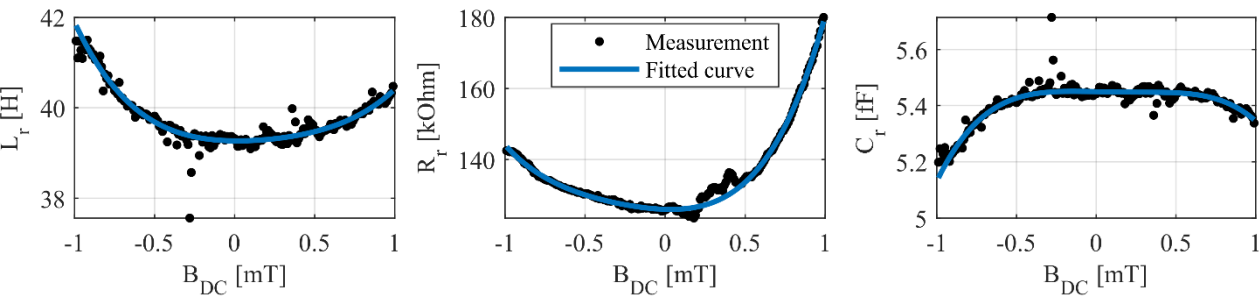


**Figure 6:** The black dots show mBvD fits found for impedance measurements at the corresponding magnetic field. The blue lines are 4<sup>th</sup> order polynomial functions approximating the behavior of the RLC tank components.

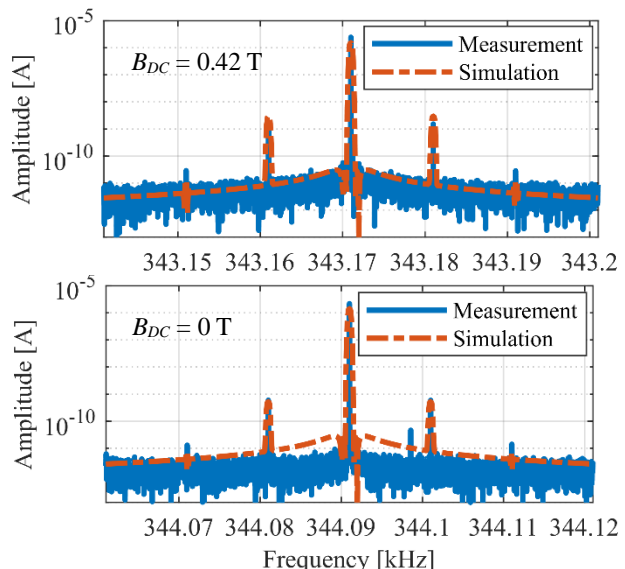


Figure 7: A comparison of signal measurements with signals somulations based on the extended mBvD model is shown. The magnetic field  $B_{DC}$  is given in the plots. An excitation frequency of  $f_{\rm ex}$  = 343,17 kHz resp.  $f_{\rm ex}$  = 344,09 kHz is used with  $u_{\rm ex}$  = 100 mV. The magnetic signal is excited at  $f_{Bac}$  = 10 Hz with an amplitude of  $B_{AC}$  = 1  $\mu$ T.

## 6 Conclusion

The presented extension to the mBvD model can be used to simulate the resonator not only in noise analysis, but also for dynamic magnetic signals at different magnetic bias points. It is planned to further extend this model by including the additional dependency of the sensor response on the excitation voltage amplitude, which is currently not modelled. The analytical model can efficiently be implemented in the future in Spice or other circuit simulators to simulate the resonator together with supporting circuitry e.g., a frequency generator or an ADC, yielding system level results for circuit designs.

#### **Author Statement**

Research funding: This work was supported by the German Research Foundation (DFG) through the Collaborative Research Center under Grant CRC 1261. Conflict of interest: Authors state no conflict of interest. Informed consent: Informed consent has been obtained from all individuals included in this study. Ethical approval: The research related to human use complies with all the relevant national regulations, institutional policies and was performed in accordance with the tenets of the Helsinki Declaration, and has been approved by the authors' institutional review board or equivalent committee.

#### References

- Ilgaz F, Spetzler E, Wiegand P, et al. Signal-noise analysis of miniaturized delta-E effect magnetic field sensors. Applied Physics Letters. 2025;126(8):084103.
- [2] Spetzler B, Bald C, Durdaut P, et al. Exchange biased delta-E effect enables the detection of low frequency pT magnetic fields with simultaneous localization. Sci Rep. 2021;11(1):5269.
- [3] Panina L, Nemirovich M. 2 Magnetic sensors for diagnosis and healthcare applications. In: Magnetic Sensors and Actuators in Medicine [Internet]. Woodhead Publishing; 2023:5–25.
- [4] Singh A, Mitra D, Mandal B, et al. A review of electromagnetic sensing for healthcare applications. AEU -International Journal of Electronics and Communications. 2023;171:154873.
- [5] Hoffmann J, Wolframm H, Engelhardt E, et al. A Magnetoelectric Distance Estimation System for Relative Human Motion Tracking. Sensors. 2025;25(2):495.
- [6] Bald C, Schmidt G. Processing Chain for Localization of Magnetoelectric Sensors in Real Time. Sensors. 2021;21(16):5675.
- [7] Jin H, Dong SR, Luo JK, et al. Generalised Butterworth-Van Dyke equivalent circuit for thin-film bulk acoustic resonator. Electronics Letters. 2011;47(7):424–426.
- [8] Ilgaz F, Spetzler E, Wiegand P, et al. Miniaturized doublewing ΔE-effect magnetic field sensors. Sci Rep. 2024;14(1):11075.
- [9] Reermann J, Zabel S, Kirchhof C, et al. Adaptive Readout Schemes for Thin-Film Magnetoelectric Sensors Based on the delta-E Effect. IEEE Sensors Journal. 2016;16(12):4891– 4900
- [10] Ludwig A, Quandt E. Optimization of the /spl Delta/E effect in thin films and multilayers by magnetic field annealing. IEEE Transactions on Magnetics. 2002;38(5):2829–2831.
- [11] Durdaut P, Reermann J, Zabel S, et al. Modeling and Analysis of Noise Sources for Thin-Film Magnetoelectric Sensors Based on the Delta-E Effect. IEEE Trans Instrum Meas. 2017;66(10):2771–2779.
- [12] Spetzler E, Spetzler B, McCord J. A Magnetoelastic Twist on Magnetic Noise: The Connection with Intrinsic Nonlinearities. Advanced Functional Materials. 2024;34(9):2309867.
- [13] Spetzler B, Wiegand P, Durdaut P, et al. Modeling and Parallel Operation of Exchange-Biased Delta-E Effect Magnetometers for Sensor Arrays. Sensors. 2021;21(22):7594.
- [14] Arnau A, Jimenez Y, Sogorb T. An extended Butterworth Van Dyke model for quartz crystal microbalance applications in viscoelastic fluid media. IEEE Transactions on Ultrasonics, Ferroelectrics, and Frequency Control. 2001;48(5):1367– 1382.
- [15] Hagmann MJ. Analysis and equivalent circuit for accurate wideband calculations of the impedance for a piezoelectric transducer having loss. AIP Advances. 2019;9(8):085313.
- [16] Jahns R, Knöchel R, Greve H, et al. Magnetoelectric sensors for biomagnetic measurements. 2011 IEEE International Symposium on Medical Measurements and Applications 2011;107–110.